Metal-oxide interfaces at the nanoscale

Guangwen Zhou[a)]
Department of Mechanical Engineering and Multidisciplinary Program in Materials Science and Engineering, State University of New York, Binghamton, New York 13902, USA

(Received 13 May 2009; accepted 22 May 2009; published online 10 June 2009)

In contrast to the 6×7 spacing registry that yields a minimum coincidence misfit, we find that the nanoscale Cu_2O-Cu interface formed during initial oxidation of Cu(111) surfaces adopts a 5×6 coincidence site lattice that is accommodated by an increased lattice misfit strain. A simple analysis on the equilibrium elastic strain in epitaxial oxide nanoislands reveals a previously unnoticed correlation between the interface structure and surface stresses at the nanoscale. © *2009 American Institute of Physics*. [DOI: 10.1063/1.3154546]

The metal-oxide interface is a crucial zone not only in the fundamental understanding of oxidation mechanism of metals but also for many technologically important processes including corrosion, catalysis, and thin film growth. Generally, the lattice parameter of an oxide is significantly larger than that of the metal from which it is formed. This large lattice misfit makes the formation of coherent metal-oxide interface energetically unfavorable although many oxides are nonetheless observed to grow crystallographically aligned with the metal substrates. A classical model describing the occurrence of epitaxy in such a large-misfit system is the coincidence site lattice (CSL) interface that requires lattice strains small enough to be energetically feasible for the heteroepitaxial growth.[1–3] In this case, the bilayer would be in a local minimum energy state if the mth atom of the overgrowth coincides with the n^{th} atom of the substrate surface layer by introducing a minimum lattice misfit $F=-(ma_o-na_s)/ma_o$ with the interface configuration determined by $a_o/a_s=m/n$; $n=m\pm1$, where a_o and a_s are the unstrained lattice constants of the oxide overlayer and the metal substrate, respectively, m and n are integers. In this work, we show that this minimum CSL misfit criterion is insufficient to predict the structure of nanoscale metal-oxide interfaces, where surface stress induced strains can significantly affect the thermodynamically predicted interface structure.

Our study is based on the oxidation of Cu, a model system to understand the mechanism of metal oxidation.[4–9] Under the conditions used in this study, Cu_2O is the stable oxide that forms on Cu, and the cubic Cu_2O lattice aligns epitaxially with the Cu lattice. The natural lattice misfit, f, between Cu and Cu_2O, defined by $f=(a_{Cu_2O}-a_{Cu})/a_{Cu_2O}$ is 15.4%, where the lattice constants of bulk Cu_2O and Cu are 4.269 and 3.61 Å, respectively. Based on the minimum CSL misfit criterion, a 6×7 CSL interface can be easily predicted at the $Cu-Cu_2O$ interface in which 6 Cu-spacings in Cu_2O overlayer exactly match 7 Cu spacings in Cu substrate. In this case, the minimum CSL strain, F, to produce the 6×7 CSL is 1.22%.[10] However, our results, obtained by high-resolution transmission electron microscopy (HRTEM), demonstrate that the nanoscale $Cu_2O-Cu(111)$ interface adopts a 5×6 CSL that is accommodated by a larger misfit strain. The correlation between surface stresses and interface structures is generally not considered in theories of heteroepitaxial growth, but is found to be of importance here. We believe that our conclusions hold generally for heteroepitaxial growth of nanostructures. This is particularly significant given the need for atomic control of the interfacial structure of ultrathin oxide films for many technological applications.

In situ oxidation and imaging/diffraction and *ex situ* HRTEM were employed in this study. *In situ* oxidation experiments were carried out in a modified ultrahigh vacuum (UHV) transmission electron microscope equipped to allow observation of oxidation in controlled oxygen pressure (for details see Ref. 11). Cu(111) single crystal films with thickness ~600 Å thickness were grown on NaCl(111) by e-beam evaporation. The Cu films were removed from the substrate by flotation in deionized water, washed, and mounted on a specially designed sample holder that allows for resistive heating. Any native Cu oxide is removed by annealing the films inside the TEM in methanol vapor at a pressure of 5×10^{-5} Torr and 350 °C (Ref. 12) or annealing under vacuum condition at ~800 °C,[13,14] which reduces the copper oxides to copper and results in clean copper surfaces. *Ex situ* HRTEM observation using a JEOL 2010F electron microscope was made immediately after removal from the UHV-TEM. Electron moiré fringe imaging was employed to determine the interface configuration of Cu_2O nanoislands with the Cu substrate. *In situ* electron diffraction in the UHV-TEM was taken before the transfer and was compared with the electron diffraction pattern in the JEOL-2010F to check the effect of sample transfer. No appreciable difference was noted.

Figure 1(a) shows an *in situ* TEM observation of the

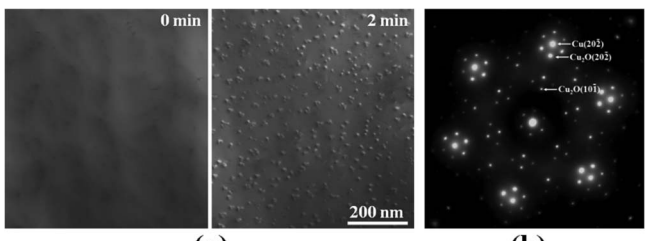

FIG. 1. (a) *In situ* TEM observation of the oxidation of a Cu(111) surface at 350 °C and $pO_2=5\times10^{-4}$ Torr. (b) Selected area electron diffraction from the oxidized Cu(111) surface reveals the epitaxial growth of Cu_2O nanoislands; additional reflections are due to double diffraction of electron beams by Cu and Cu_2O.

a)Author to whom correspondence should be addressed. Electronic mail: gzhou@binghamton.edu.

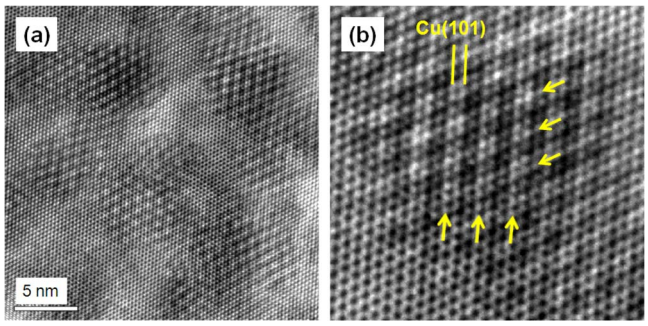

FIG. 2. (Color online) (a) Cu(111) lattice fringes and electron moiré fringes due to the lattice superimposition of Cu_2O islands and the Cu substrate. (b) Enlarged view of the moiré fringes, which clearly reveals that each moiré repeat contains three Cu(101) spacings.

oxidation of a Cu(111) surface at 350 °C and oxygen pressure of 5×10^{-4} Torr. After introduction of O_2, oxide nuclei appeared quickly on the clean Cu surface. Oxide islands have a random distribution and relatively uniform size and the island height is ~2.5 nm as known by *ex situ* atomic force microscopy. *In situ* electron diffraction [Fig. 1(b)] was used to determine the orientation of oxide islands with the substrate. Indexing of the diffraction pattern identifies one set of reflections are from the Cu(111) substrate and the other set is from Cu_2O islands. Satellite diffraction spots appearing around the basic reflections of Cu_2O and Cu are the result of double diffraction of electron beams by the (202) planes of Cu_2O and Cu substrate. The electron diffraction pattern indicates that Cu_2O islands are epitaxial with the Cu(111) substrate, i.e., $[111]_{Cu_2O}\|[111]_{Cu}$ and $(20\bar{2})_{Cu_2O}\|(20\bar{2})_{Cu}$.

Figure 2(a) shows a plan-view HRTEM image of an oxidized Cu(111) surface viewed along the [111] zone axis. The regions with Cu_2O islands show moiré fringe contrast formed as a result of interference between diffracted beams from overlapping Cu_2O nanoislands and the Cu substrate. An obvious feature in the HRTEM image is that moiré fringes do not extend continuously to the entire surface, confirming the oxide island growth mode during early stages of Cu oxidation. Regions between Cu_2O islands have the lattice spacing consistent with the interplanar spacing of Cu{101}.

Electron moiré fringe contrast has been extensively used to study epitaxial growth for its sensitivity to strain and orientation and allows the elucidation of interface structures.[15–19] We use electron moiré fringe imaging to determine the interface configuration between Cu_2O nanoislands and the Cu(111) substrate. The presence of moiré fringes indicates a mismatch in the lattice spacing of the two crystals; therefore, the oxide-substrate interface cannot be coherent. Figure 2(b) shows an enlarged view of the moiré fringes with the [111] orientation. The moiré fringes run parallel to {101} planes of the Cu substrate, suggesting that the in-plane spacings of Cu_2O islands are aligned with the equivalent planes of the substrate and the moiré fringes are pure translation type. The in-plane alignment between Cu_2O islands and the Cu substrate can also be confirmed by absence of arc-like diffraction spots in Fig. 2 (arclike diffraction spots can be used to check the azimuthal distribution of nanoclusters during heteroepitxial growth[15,20]).

Figure 2(b) clearly reveals that each repeat of the moiré fringes contains 3 Cu{101} planes for the $[111]_{Cu_2O}\|[111]_{Cu}$ epitaxy. The contribution to the moiré fringe contrast in the HRTEM images comes from double diffraction of (202) reflections from Cu_2O islands and the Cu substrate because of the systematic absence of Cu(101) reflection. Therefore, each moiré repeat contains 6 Cu{202} planes. For moiré fringes generated by two sets of planes across an interface with spacing d_1 and d_2, the number of planes n of spacing d_2 between the moiré repeat is given by $n=d_2/(d_1-d_2)$, where $d_1>d_2$.[18,21] Substituting $n=6$ and the lattice spacing of Cu(202) ($d_2=1.275$ Å), the interplanar spacing of $Cu_2O(202)$ (d_1) is determined to be 1.487 Å. This gives the lattice constant of $a_{Cu_2O}=4.206$ Å and a compressive strain of 1.48%. Moiré fringes are known to be very sensitive to strain and give a better measurement of epitaxial strain than electron diffraction.[16] The number of {202} planes of Cu_2O (with spacing d_1) in a moiré repeat is calculated as nd_2/d_1, which is 5. Thus, at the Cu_2O–Cu interface, every five {202} planes in Cu_2O nanoislands match six {202} planes of the Cu substrate with a compressive coincidence strain of 1.48%. Note that the Cu substrate is taken to be rigid and the strain is mainly accommodated by Cu_2O islands. This is valid as Cu is much stronger than Cu_2O (the Young's moduli of Cu and Cu_2O are 124 and 30 GPa, respectively).

According to the coincidence epitaxy theories,[1–3] the most energetically favorable interface configuration in large-misfit systems is the one with the minimum coincidence misfit. The 6×7 CSL is the expected Cu_2O–Cu interface structure because it provides the minimum coincidence misfit of $F_0=1.22\%$. Selection of the 5×6 CSL between Cu_2O nanoislands and the Cu substrate does not fit within this criterion. In order to understand this apparent deviation, we analyze the equilibrium strain in epitaxial oxide nanoislands by incorporating surface stress effects, which become significant in the small size regime. A standard approach to understanding the equilibrium strain state in an island during epitaxial growth has been to minimize, with respect to the epitaxial strain, the sum of the volume strain energy of the island and the energy of the island-substrate interface. However, this traditional approach ignores the strain energy associated with the free surface of the island, which can affect the equilibrium state of the system, especially for small islands. In order to elucidate the effect of surface stresses on the modification of the metal-oxide interface, we consider the formation energy of an epitaxial island by incorporating the energy contribution from surface stresses. The energy change per unit area for the formation of an epitaxial island can be obtained as

$$U=\frac{2G_o(1+v)}{1-v}\varepsilon^2h+\frac{G_oG_sb|F-\varepsilon|}{\pi(G_o+G_s)(1-v)}\left[\ln\left(\frac{h}{b}\right)+1\right]+2\int f d|\varepsilon|, \quad (1)$$

where ε is the elastic strain in the island, G_o and G_s are the shear moduli of the oxide island and the substrate, respectively, ν is Poisson's ratio, F is the total lattice misfit, b is the edge component of the Burgers vector of misfit dislocations, h is island thickness, and f is the net surface stress. The first term in Eq. (1) is the volume strain energy in the elastically strained island; the second is related to the misfit dislocation energy;[1] and the third represents the strain energy associated with the surface stress, in which f can be taken to be isotropic and independent of ε for simplicity.[22] The magnitude of

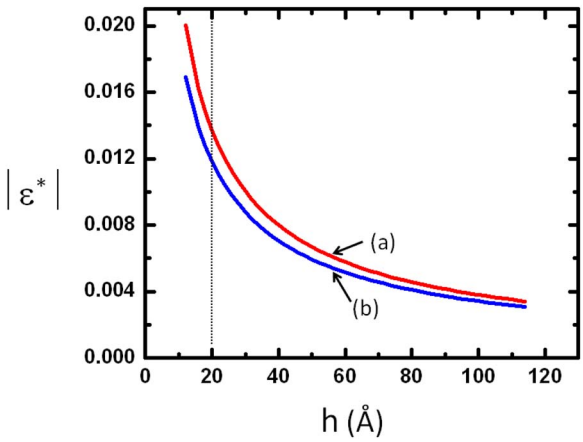

FIG. 3. (Color online) The equilibrium strain state ε^* as a function of island thickness h: (a) the surface stress effect is included and (b) no surface stress effect included. The dashed line indicates the island thickness in this work.

the equilibrium elastic strain ε^* at which the total energy U is a minimum can be obtained by setting $\partial U/\partial\varepsilon=0$,

$$|\varepsilon|^* = \frac{G_s b}{4\pi(G_s+G_o)(1+\upsilon)h}\left[\ln\left(\frac{h}{b}\right)+1\right] \pm \frac{f(1-\upsilon)}{2G_o(1+\upsilon)h}, \tag{2}$$

where "+" is for the system having a compressive strain and "−" is for a tensile strain.

Figure 3 depicts the equilibrium strain $|\varepsilon^*|$ as a function of island thickness using the following values: $G_{Cu_2O}=10$ GPa, $G_{Cu}=40$ GPa, $\upsilon=0.455$, and $b=1.5$ Å. The exact value of f for Cu_2O is not readily available in the literature and we use a typical number of $f=1$ J/m^2 for ionic solids.[23] Curve (a) is obtained using Eq. (2) where the surface stress effect is included. For comparison, curve (b) shows the equilibrium strain ε^* without the surface stress effect included. As can be seen in the plot, inclusion of a surface stress has the effect of increasing the equilibrium strain ε^* for small island thickness. For 2 nm thick islands as measured in this work, the difference in CSL misfit due to the effect of surface stresses is $\Delta\varepsilon=\sim 0.2\%$, which is very close to our measurements. This explains why the buried interface of Cu_2O nanoislands adopts the 5×6 CSL rather than the 6×7 CSL although the latter offers a smaller coincidence lattice misfit. The surface stress can also influence the oxide growth mechanism through modifying the metal-oxide lattice mismatch. The increased lattice strain between the Cu_2O and the Cu substrate leads to a larger interface energy, which drives the oxide islanding growth mode, thereby reducing the Cu_2O–Cu interface area.

The effect of surface stresses on modification of the equilibrium strain in Cu_2O nanoislands can be understood physically by considering a system responding to a competition between surface and volume effects. During the formation of Cu_2O nanoislands, the oxide is elastically compressed in order to accommodate some of the CSL misfit. Additionally, the effect of the surface stress, which favors the reduction of surface area, is also important due to the large ratio of surface to volume for small islands. The compressive surface stress causes the oxide lattice to contract further and thus produces additional lattice strain in oxide islands. For thick oxide islands, the volume strain, which favors the bulk equilibrium lattice spacing, becomes dominant. This feature can be noted in Fig. 3, where curve (a) approaches curve (b) with increasing island height due to the diminishing effect of surface stresses for thick islands. For instance, the surface stress effects cause only 0.03% of difference in the CSL misfit for 10 nm thick islands and the normal 6×7 CSL is then expected. This trend is also consistent with the synchrotron x-ray measurement of the lattice strain of Cu_2O films on Cu(111), which indicates that the in-plane lattice spacing approaches the bulk cuprite spacing as the oxide film grows thicker.[24] Further comparison between experiments and the theory can be made by comparing the interface configuration of thinner oxide islands or the oxidation of other metal substrates such as Cu(100) or (110).

In conclusion, we have shown that the interface configuration between Cu_2O nanoislands and Cu substrates deviates from the prediction based on the minimum coincidence lattice misfit criterion. Calculation of the equilibrium strain in epitaxial oxide nanoislands reveals the previously unnoticed correlation between the interface structure and surface stress effects at the nanoscale. The insights obtained from this study are expected to have broader implications in understanding and controlling the interfacial atomic structures in heteroepitaxial growth of nanostructures.

The author would like to thank Professor Judith C Yang for help for the performance of this work. The author gratefully acknowledges support from the National Science Foundation (NSF) under the Grant No. CMMI-0825737.

[1] J. W. Matthews, in *Epitaxial Growth, Part B*, edited by J. W. Matthews (Academic, New York, 1975).
[2] N. Fletcher and P. L. Adamson, Philos. Mag. **14**, 99 (1966).
[3] W. Bollmann, *Crystal Defects and Crystalline Interfaces* (Springer, Berlin, 1970).
[4] R. H. Milne and A. Howie, Philos. Mag. A **49**, 665 (1984).
[5] J. C. Yang, B. Kolasa, J. M. Gibson, and M. Yeadon, Appl. Phys. Lett. **73**, 2841 (1998).
[6] J. A. Eastman, P. H. Fuss, L. E. Rehn, P. E. Baldo, G. W. Zhou, D. D. Fong, and L. J. Thompson, Appl. Phys. Lett. **87**, 051914 (2005).
[7] M. Lampimaki, K. Lahtonen, M. Hirsimaki, and M. Valden, J. Chem. Phys. **126**, 034703 (2007).
[8] K. Lahtonen, M. Hirsimaki, M. Lampimaki, and M. Valden, J. Chem. Phys. **129**, 124703 (2008).
[9] G. W. Zhou, X. D. Chen, D. Gallagher, and J. C. Yang, Appl. Phys. Lett. **93**, 123104 (2008).
[10] J. H. Ho and R. W. Vook, J. Cryst. Growth **44**, 561 (1978).
[11] M. L. McDonald, J. M. Gibson, and F. C. Unterwald, Rev. Sci. Instrum. **60**, 700 (1989).
[12] S. M. Francis, F. M. Leibsle, S. Haq, N. Xiang, and M. Bowker, Surf. Sci. **315**, 284 (1994).
[13] G. W. Zhou and J. C. Yang, Phys. Rev. Lett. **93**, 226101 (2004).
[14] G. W. Zhou, W. Y. Dai, and J. C. Yang, Phys. Rev. B **77**, 245427 (2008).
[15] B. Q. Li and J. M. Zuo, Surf. Sci. **520**, 7 (2002).
[16] J. M. Zuo and B. Q. Li, Phys. Rev. Lett. **88**, 255502 (2002).
[17] Y. Ding, X. Y. Kong, and Z. L. Wang, J. Appl. Phys. **95**, 306 (2004).
[18] K. Chatterjee, J. M. Howe, W. C. Johnson, and M. Murayama, Acta Mater. **52**, 2923 (2004).
[19] Y. J. Geng and M. G. Norton, J. Mater. Res. **14**, 2708 (1999).
[20] B. Q. Li and J. M. Zuo, J. Appl. Phys. **94**, 743 (2003).
[21] P. B. Hirsch, A. Howie, R. B. Nicholson, D. W. Pashley, and M. J. Whelan, *Electron Microscopy of Thin Crystals* (Krieger, New York, 1977).
[22] R. C. Cammarata and K. Sieradzki, Appl. Phys. Lett. **55**, 1197 (1989).
[23] R. C. Cammarata, Prog. Surf. Sci. **46**, 1 (1994).
[24] Y. S. Chu, I. K. Robinson, and A. A. Gewirth, J. Chem. Phys. **110**, 5952 (1999).